

Receptor tyrosine kinase ErbB4 modulates neuroblast migration and placement in the adult forebrain

E S Anton^{1,8}, H T Ghashghaei^{1,8}, Janet L Weber², Corey McCann¹, Tobias M Fischer², Isla D Cheung², Martin Gassmann³, Albee Messing⁴, Rudiger Klein⁵, Markus H Schwab^{2,6}, K C Kent Lloyd⁷ & Cary Lai²

Neural progenitor proliferation, differentiation and migration are continually active in the rostral migratory stream of the adult brain. Here, we show that the receptor tyrosine kinase ErbB4 is expressed prominently by the neuroblasts present in the subventricular zone and the rostral migratory stream. The neuregulins (NRG1–NRG3), which have been identified as ErbB4 ligands, are detected either in the stream or in adjacent regions. Mice deficient in ErbB4 expressed under the control of either the nestin or the hGFAP promoter have altered neuroblast chain organization and migration and deficits in the placement and differentiation of olfactory interneurons. These findings suggest that ErbB4 activation helps to regulate the organization of neural chains that form the rostral migratory stream and influences the differentiation of olfactory interneuronal precursors.

The ability of the mature mammalian nervous system to produce neuronal precursors continually is of considerable importance, as manipulation of this process might one day permit the replacement of cells lost as a result of injury or disease. In the rodent brain, the anterior region of the lateral ventricle and the hippocampus are the primary sites of adult neurogenesis^{1–3}. Neural progenitor cells born in the subventricular zone (SVZ), the mitotically active region immediately adjacent to the anterior lateral ventricle, migrate towards the olfactory bulb (OB), forming a structure called the rostral migratory stream (RMS), which contains cells destined to become olfactory interneurons^{1,4,5}. These neural precursors migrate tangentially in a chain-like structure, maintaining contact with other migrating cells, but in the absence of radial glial or axonal guides¹. These cells seem to move through tube-like structures formed by a cell type that expresses the astrocytic marker glial fibrillary acidic protein (GFAP) and nestin, a marker of neural precursors. The nestin⁺ GFAP⁺ cells give rise to a third, rapidly proliferating cell type (nestin⁺ dlx-2⁺) located in the SVZ, which in turn gives rise to the migrating neuronal precursors in the stream^{1,5,6}. These three cell types are believed to derive from a distinct GFAP⁺ or LeX⁺ primary neural stem cell^{1,7,8}. The identification of factors that promote neural stem cell division and that regulate the proliferation, migration and differentiation of their progeny would facilitate attempts to manipulate the production of new neurons and glia and help in understanding the ongoing maintenance of neural circuitry in the mature CNS.

In vitro and *in vivo*, multiple factors, including the brain-derived neurotrophic factor, insulin-like growth factor-1, erythropoietin, epidermal growth factor (EGF) and the basic fibroblast growth factor, have been shown to support the production of neural cells from SVZ cells^{6,9–11}.

Mice that lack the EGF receptor (EGFR) and its ligand, transforming growth factor- α (TGF- α), undergo early postnatal neurodegeneration of the forebrain and have fewer proliferating cells in the SVZ^{12,13}.

The EGFR is structurally most closely related to three other receptor protein-tyrosine kinases, ErbB2, ErbB3 and ErbB4 (ref. 14), which can be activated by multiple EGF-like domain-containing ligands, including the neuregulins (NRGs). The NRGs are best known for their ability to induce the transcription of genes encoding acetylcholine receptor subunits (acetylcholine receptor-inducing activity) and other components of the postsynaptic neuromuscular junction in muscle cells grown *in vitro*¹⁵. A recent report has provided evidence that a subset of NRG isoforms are required for muscle spindle formation, identifying a crucial role for NRG as a differentiation factor for proprioceptive neurons¹⁶. NRG has also been characterized as a factor essential for the development of the Schwann cell and oligodendroglial lineages¹⁷, and recent studies have shown that it is a key regulator of myelin sheath thickness in the periphery¹⁸. NRG has been detected in the basal forebrain, cortex and cerebellum¹⁹, where it may have an acetylcholine receptor-inducing activity or similar role by regulating the expression of multiple ligand-gated ion channel subunits¹⁵. NRG has also been shown to affect neuronal migration on radial glial guides in cerebellum and cerebral cortex through ErbB4 and ErbB2 receptors, respectively^{20–22}.

The analysis of NRG and ErbB function in the nervous system has been complicated by the identification of multiple NRG-like ligands, including NRG2, NRG3 and NRG4 (ref. 14). NRG1–NRG3 are expressed in the mature CNS and all four NRGs activate ErbB4. We were therefore interested in determining whether activation of ErbB4 might have a role

¹UNC Neuroscience Center and the Department of Cell and Molecular Physiology, The University of North Carolina School of Medicine, Chapel Hill, North Carolina 27599, USA. ²Department of Neuropharmacology, The Scripps Research Institute, 10550 N. Torrey Pines Road, La Jolla, California 92037, USA. ³Department of Physiology, Biozentrum/Pharmazentrum, University of Basel Klingelbergstr. 50, CH-4056 Basel, Switzerland. ⁴Waisman Center on Mental Retardation & Human Development, University of Wisconsin-Madison, Madison, Wisconsin 53705-2280, USA. ⁵Max-Planck-Institut für Neurobiologie, Am Klopferspitz 18A, 82152 Martinsried, Germany. ⁶Max-Planck-Institut für Experimentelle Medizin, Hermann-Rein-Str. 3, 37075 Göttingen, Germany. ⁷Center for Comparative Medicine, School of Veterinary Medicine, University of California, Davis, One Shields Avenue, Davis, California 95616, USA. ⁸These authors contributed equally to this work. Correspondence should be addressed to E.S.A. (anton@med.unc.edu).

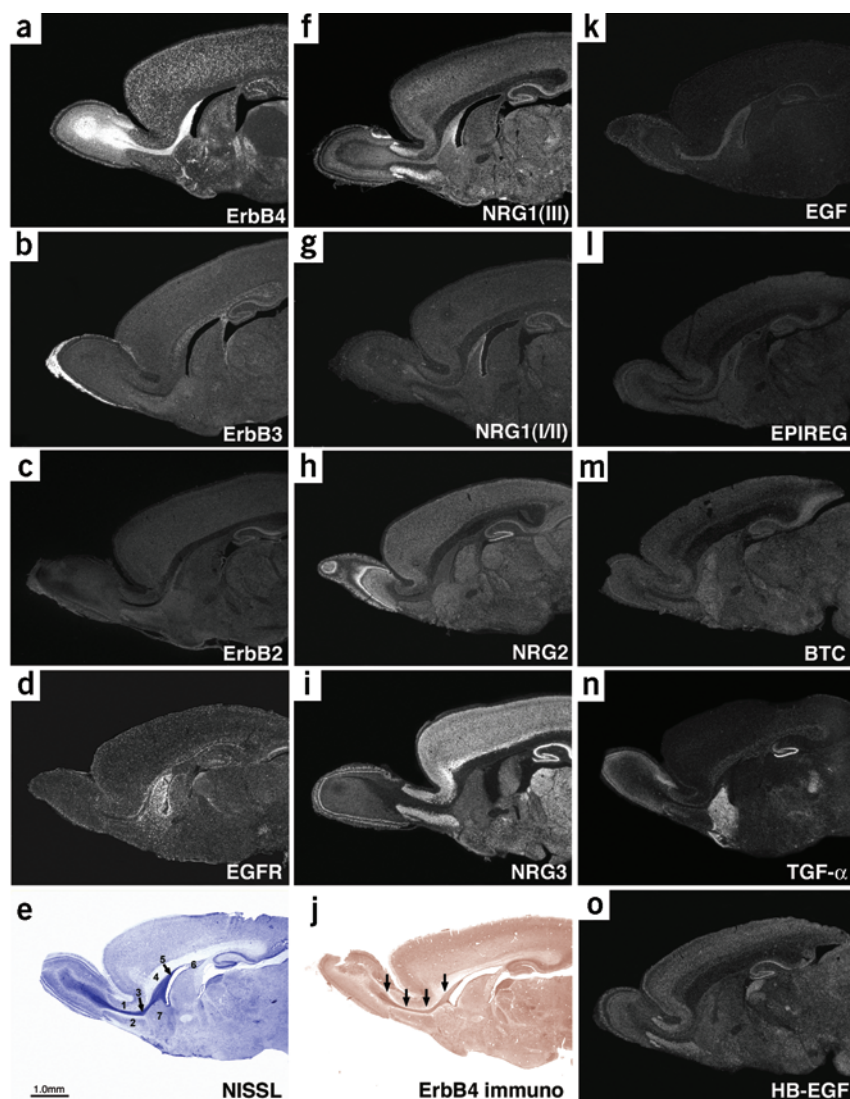


Figure 1 *In situ* localization of ErbB receptors and their ligands in the P11 rat brain. Darkfield photomicrographs of 30-μm sagittal sections of the forebrain region, which includes the RMS and SVZ. All probes were amplified from rat brain cDNA. Emulsion-dipped slides were developed 2–5 weeks after dipping. (a) ErbB4. (b) ErbB3. (c) ErbB2. (d) EGFR. (e) Nissl-stained section. (f) NRG1, SMDF or type III isoform. (g) NRG1, Ig-specific probe (types I and II). (h) NRG2. (i) NRG3. (j) Immunocytochemical staining using an affinity-purified rabbit polyclonal antiserum to ErbB4 (arrows indicate the RMS). (k) EGF. (l) EPIREG. (m) Betacellulin (BTC). (n) TGF-α. (o) HB-EGF. In e: 1, anterior olfactory nucleus, dorsal; 2, anterior olfactory nucleus, ventral; 3, RMS; 4, corpus callosum; 5, SVZ; 6, lateral ventricle; 7, striatum. Sections were prepared from 2–5 rats per probe.

also expressed in scattered cells in the striatum. EGFR is expressed in a more limited set of cells in the RMS than is ErbB4, which is uniformly distributed throughout the RMS (**Fig. 1d**). At P11, ErbB2 is faintly detected in the RMS and in the anterior lining of the lateral ventricle (**Fig. 1c**) but is more noticeable in the regions immediately adjacent to the RMS. ErbB3 is not detected in either the RMS or the lining of the ventricles but is prominent in the olfactory nerve layer of the OB and in the overlying corpus callosum (**Fig. 1b**).

In adults, EGFR- and ErbB4-specific hybridization in the RMS were lower than in P11 rats, whereas ErbB2 was more readily detected than at P11 (**Supplementary Fig. 1** online). The pattern of ErbB3 expression in adults was qualitatively similar to that seen at P11. EGFR was expressed in a subset of RMS cells and was also detected at high levels in the lining of the most anterior region of the lateral ventricle (**Supplementary Fig. 1** online).

In addition to ErbB4 mRNA, ErbB4 protein was also detected in the RMS both at P11 and in the adult (**Fig. 1j** and **Supplementary Fig. 1** online), as an affinity-purified antiserum to ErbB4 stained the SVZ and the full extent of the RMS. To determine which cell types in the RMS expressed ErbB4, we carried out double-label immunostaining with antibodies to ErbB4 and antibodies to either the polysialylated form of the neural cell adhesion molecule (PSA-NCAM), which marks the migrating cells (A cells), or to GFAP, which marks the glial tubes through which the A cells transit and a subset of neural stem cells^{5,8}. These studies showed a near-perfect colocalization of ErbB4 and PSA-NCAM in the adult RMS, indicating that this receptor was expressed by the migrating neuroblast subpopulation (**Fig. 2a–c**). ErbB4 was also detected in a small subset of GFAP⁺ glial cells dispersed in the RMS (**Fig. 2d–f**). In the SVZ, a subset of ErbB4⁺ cells colocalized with GFAP near the lateral ventricle wall (**Fig. 2g–i**). ErbB4 was also detected in a specialized subset of dlx-2⁺ cells in the SVZ. dlx-2 marks the rapidly dividing C cells and the migrating A cells of the RMS⁶ (**Fig. 2j–l**). Colocalization of dlx-2 and ErbB4 is limited in the SVZ, but more prevalent in the migrating A cells in the RMS (data not shown). ErbB4 showed limited colocalization with the carbohydrate marker LeX (also called SSEA-1), which marks a subset of neural progenitor cells⁷ (**Fig. 2m–o**).

in the proliferation, migration and differentiation of neural progenitors in the adult forebrain.

Our studies showed that ErbB4 is the predominant ErbB receptor expressed by neuroblasts in the SVZ and RMS, and that multiple ErbB4 ligands are detected in the SVZ, RMS and nearby regions. Cre-loxP-mediated inactivation of ErbB4 resulted in disorganized neuronal chains in the SVZ. SVZ explants prepared from mutant mice had a reduced ability to support the chain-like migration of neural precursors *in vitro*. The loss of ErbB4 also resulted in aberrant changes in the placement, number and phenotype of distinct subclasses of OB interneurons. These findings suggested that ErbB4 regulates neural progenitor cell migration and may influence their differentiation in the adult forebrain.

RESULTS

NRG and ErbB expression in the RMS

The expression of the ErbB receptors in the RMS and SVZ of the forebrain of postnatal day (P) 11 and adult rats was determined using *in situ* hybridization (**Fig. 1** and **Supplementary Fig. 1** online). At P11, ErbB4 is expressed at high levels in the RMS and remains detectable in these cells as they migrate into the OB (**Fig. 1a**). Expression persists in granule neurons in the mature OB, but at reduced levels. ErbB4 is

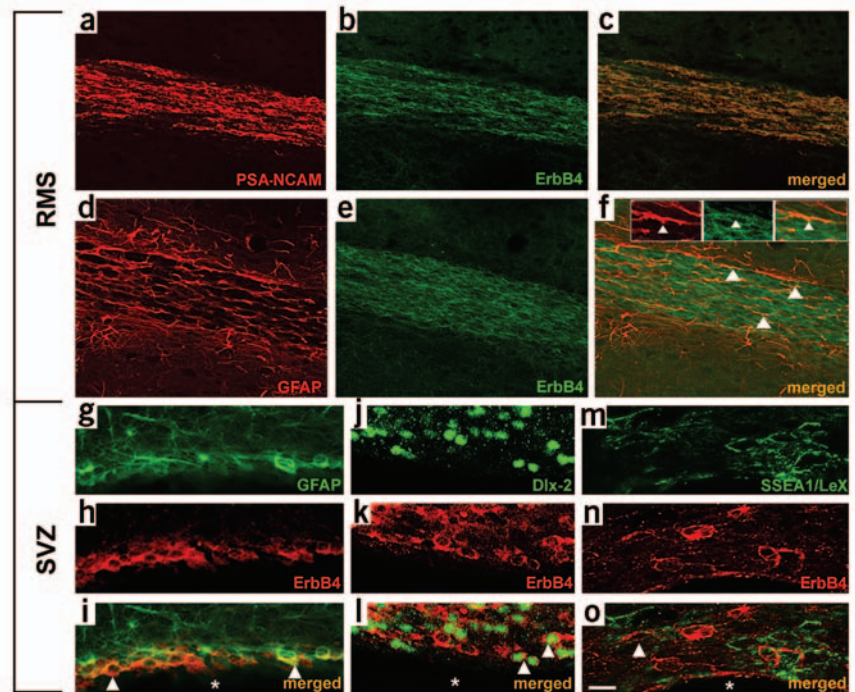


Figure 2 ErbB4 expression in the RMS and SVZ. (a–c) In sagittal sections of adult rat brain, PSA-NCAM (a) and ErbB4 (b) show a substantial degree of colocalization (c). ErbB4 (e, h) is only detected in a small subset of GFAP⁺ cells (d, g) in the RMS (arrowheads in merged image, f) and in the SVZ (merged image, i). Inset (f) shows colabeled GFAP⁺ strands at higher magnification. In the SVZ, adjacent to the ventricles, some of the dlx-2⁺ (j) and LeX⁺ (m) precursors coexpressed ErbB4 (arrowheads, l, o). (j) Anti-dlx-2. (m) Anti-LeX. (k, n) Anti-ErbB4. (l, o) Merged images. Asterisks (i, l, o) denote ventricles. Scale bars: a–f, 50 μ m; g–o, 25 μ m.

We then determined which of the ErbB4 ligands were detectable in the RMS and nearby regions (**Fig. 1** and **Supplementary Fig. 1** online). Two different classes of NRG1 isoforms were assessed, one corresponding to the immunoglobulin-like domain-containing forms (types I and II) and the other to the cysteine-rich/SMDF domain-containing forms (type III)¹⁵. The type I and II isoforms were detected at low levels in the stream both at P11 and in the adult and were also observed in the anterior lining of the ventricle at P11 (**Fig. 1g** and **Supplementary Fig. 1** online). The type III form was expressed at much higher levels than the type I and II isoforms in the RMS at P11 and was particularly noticeable in the regions surrounding the RMS, including in the anterior olfactory nucleus (**Fig. 1f**). NRG1 type III was also detected in the internal granule cell layer, as well as in the mitral cell and glomerular layers in the OB (**Fig. 1f**). In the adult, the type III isoform was detected in the same regions, but at reduced levels (**Supplementary Fig. 1** online). NRG2 was present at very low levels in the stream and at high levels in the internal granule cell, external plexiform and glomerular layers of the OB at P11 and in the adult (**Fig. 1h** and **Supplementary Fig. 1** online). NRG3 was not detected in the stream either at P11 or in the adult, but was expressed at high levels throughout the cortex, in the dorsal and ventral portions of the anterior olfactory nucleus and in the mitral and glomerular layers in the OB (**Fig. 1i** and **Supplementary Fig. 1** online). NRG4 has not yet been detected at appreciable levels in the nervous system (J.L.W., unpublished observations).

In addition, we assessed the levels of other potential ligands, including betacellulin, heparin-binding EGF (HB-EGF) and ependymin, which activate both ErbB4 and EGFR^{14,23} (**Fig. 1l, m, o** and **Supplementary Fig. 1** online), and EGF and TGF- α (**Fig. 1k, n** and **Supplementary Fig. 1** online), which activate EGFR but not ErbB4 (ref. 23). Of these, EGF was detected in both the RMS and the anterior lining of the lateral ventricle (**Fig. 1k**), whereas TGF- α was detected at high levels in the striatum but at low levels in the adult RMS and in an adjacent white matter tract, the intrabulbar anterior commissure (**Fig. 1n** and **Supplementary Fig. 1** online).

These studies showed that ErbB4 is expressed by the migrating neuroblasts and at least some of the proliferating precursors of the SVZ. Multiple potential ligands, including three of the NRGs, are located in the forebrain region, where they may influence neuroblast proliferation, migration and differentiation through ErbB4.

Conditional deletion of ErbB4 disrupts RMS organization

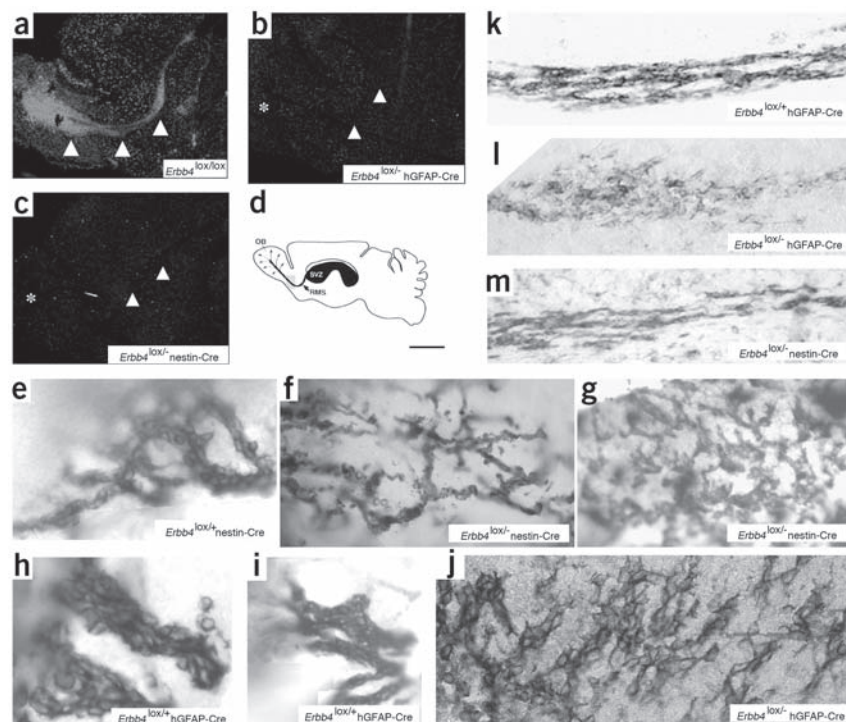
We then generated lines of conditional null mice that lacked ErbB4 expression in the CNS to evaluate the role of this receptor in the SVZ and RMS. We mated mice in which the second exon of the gene *ErbB4* was flanked by loxP sites²⁴ with transgenic mice that expressed Cre recombinase under the control of either the human GFAP (hGFAP) promoter or the rat nestin promoter and enhancer.

To maximize the number of cells with a complete loss of ErbB4 function, we mated the mice carrying loxP sites (*ErbB4*^{lox/−}) with the mice

carrying Cre recombinase in a background that is heterozygous with respect to the null allele of *ErbB4* (*ErbB4*^{−/−}; ref. 25). Mating these mice to the nestin-Cre line²⁶ resulted in transgenic mice deficient in ErbB4 expression in nestin⁺ neuronal precursor cells (*ErbB4*^{lox/−} nestin-Cre). The nestin-Cre transgene induces widespread recombination of the reporter genes Rosa26lacZ^{lox} and β 1-integrin^{lox} (ref. 27) in the CNS beginning around embryonic day (E) 10.5. Similarly, we inactivated ErbB4 in cells in which the hGFAP promoter is active, which includes many astrocyte-like cells. The hGFAP promoter is active in neural progenitors as early as E13.5 (ref. 28); therefore, Cre-mediated recombination occurs widely throughout the developing brain in these mice (*ErbB4*^{lox/−} hGFAP-Cre). *In situ* hybridization using a probe specific to *ErbB4* exon 2 did not detect any cells in either the RMS or the OB of P12 *ErbB4*^{lox/−} nestin-Cre or *ErbB4*^{lox/−} hGFAP-Cre mice (**Fig. 3a–c**). Evidence for the loss of ErbB4 expression was also obtained using antibodies to ErbB4 (**Supplementary Fig. 2** online).

In vivo, the structure of the SVZ in the regions adjacent to the lateral ventricles in the *ErbB4*^{lox/−} nestin-Cre and *ErbB4*^{lox/−} hGFAP-Cre mice were considerably disorganized compared with those of littermate controls (**Fig. 3d–j**). This difference in morphology was visualized using antibodies to PSA-NCAM, which mark neuroblasts that are typically organized as clusters of chains in the RMS and SVZ. The PSA-NCAM⁺ cells in the mutant mice formed fragmented chains that did not have the normal interdigitated and contiguous appearance (**Fig. 3f–j**). TUNEL labeling analyses of the SVZ of control or ErbB4-conditionally null mice identified no substantial differences between groups (data not shown). In addition to these changes observed near the ventricle wall, when viewed at low magnification, the RMS of *ErbB4*^{lox/−} hGFAP-Cre mice

Figure 3 Altered RMS in conditional mutants of ErbB4. (**a–d**) Nestin-Cre-mediated or hGFAP-Cre-mediated recombination was used to inactivate ErbB4 expression in the RMS. (**a**) *In situ* hybridization using a probe specific for exon 2 of ErbB4 indicated that in control mice, ErbB4 was readily detected throughout the RMS, but was not detectable in the RMS after hGFAP-Cre-mediated (**b**) or nestin-Cre-mediated (**c**) recombination of *ErbB4*^{lox} alleles. The asterisks denote the OB region; arrowheads denote ventral boundaries of the RMS. (**d**) Sagittal view of mature brain to illustrate the SVZ, RMS and OB (adapted from ref. 5). (**e–j**) SVZ region. (**k–m**) Mid-RMS region, highlighted by the gray box shown in **d**. (**e–j**) The RMS was labeled with antibodies to PSA-NCAM in control mice (*ErbB4*^{lox/+} nestin-Cre, **e**; *ErbB4*^{lox/+} hGFAP-Cre, **h,i**) or mice deficient in ErbB4 expression in the nervous system (*ErbB4*^{lox/-} nestin-Cre, **f,g**; *ErbB4*^{lox/-} hGFAP-Cre, **j**). The structure of the SVZ in the regions adjacent to the anterior lateral ventricles in the *ErbB4*^{lox/-} nestin-Cre mice (**f,g**) were considerably disorganized and fragmented compared to controls (**e**). Similar disorganization of contiguous chains was observed in *ErbB4*^{lox/-} hGFAP-Cre mice (**j**). (**k–m**) As neuroblasts migrate away from the SVZ, they normally form a tightly clustered stream with smooth boundaries as they course towards the OB (**k**). In *ErbB4*^{lox/-} hGFAP-Cre mice, however, the cells are less tightly grouped in the RMS, giving rise to a loosely organized stream of cells that has noticeably jagged boundaries (**l**). Less prominent disorganization was also seen in *ErbB4*^{lox/-} nestin-Cre mice (**m**). Upper left corner of **e–j** is towards the ventricle. Orientation of **k–m**: to the left is towards the SVZ, to the right is towards the OB. PSA-NCAM analysis is based on sections prepared from 8–10 adult mice per group. Scale bars: **a–c**, 700 μ m; **d**, 5 mm; **e–m**, 80 μ m.



had a noticeably jagged boundary with the surrounding tissue (**Fig. 3l**) relative to controls (**Fig. 3k**). A similar, but less pronounced deficit was also noticed in the *ErbB4*^{lox/-} nestin-Cre mice (**Fig. 3m**). To determine how these gross morphological differences were reflected at the cellular level, we carried out electron microscopic ultrastructural analyses using 1.0- μ m-thick sections of the RMS. In general, the close apposition of migrating cells (A cells) and the glial-like cells (B1, B2) that normally ensheath them was greatly reduced in the *ErbB4*^{lox/-} hGFAP-Cre mice (**Fig. 4**). Thus, the loss of ErbB4 seems to disrupt the characteristic 'glial tube' organization found in the normal adult RMS¹.

To determine how the loss of ErbB4 signaling affected neural precursor migration *in vitro*, we cultured SVZ explants from mutant and control mice in gel matrix and the patterns of migration were assessed (**Supplementary Fig. 3** online). Both *ErbB4*^{lox/-} nestin-Cre and *ErbB4*^{lox/-} hGFAP-Cre explants yielded primarily isolated migrating cells but also gave rise to loosely formed, fragmented chains. In contrast, cells emigrating from control explants formed compact neuronal chains (**Supplementary Fig. 3** online). Taken together, these results from mice that lack ErbB4 in neural precursors were indicative of an *in vivo* requirement for ErbB4 for the formation and organization of the RMS.

ErbB4 modulates neuroblast migration *in vivo*

We then directly examined RMS neuroblast migration in mutant (*ErbB4*^{lox/-} hGFAP-Cre) and control mice. To visualize migrating cells, we labeled neuroblasts at their site of origin in the anterior SVZ using intraventricular injections of the cell-tracker dye CMTMR and allowed them to migrate into the stream for 4–6 h. Forebrain slices were then prepared, and migrating neuroblasts in the stream were monitored in

real time by confocal microscopy. Neuroblasts migrated in an oriented manner towards the OB, at a rate of $49.29 \pm 6.14 \mu\text{m h}^{-1}$ (**Fig. 5a,b**). These cells were observed to "slide along each other", as previously described²⁹. In contrast, ErbB4-null cells migrated at a significantly slower rate ($26.30 \pm 3.58 \mu\text{m h}^{-1}$) and in more varied orientations (**Fig. 5a,b**). The migrating cells in the mutant RMS were morphologically distinguishable from those in control cells, which had a long leading process oriented towards the OB and a short trailing process (**Fig. 5c**). ErbB4-null neuroblasts lacked these oriented processes: their leading processes were directed in multiple orientations (**Fig. 5c**). To evaluate the changes in the orientation of migration, we used live-cell imaging to quantify the number of neuroblasts moving towards the OB, towards the SVZ or perpendicular to the RMS towards the surrounding parenchyma (**Fig. 5d**). In the control RMS, most ($79\% \pm 2.46\%$; mean \pm s.e.m.) of the neuroblasts moved towards the OB, with $\sim 15\%$ ($\pm 1.4\%$) moving in the opposite direction (towards the SVZ) and 6% ($\pm 1.51\%$) moving perpendicular to the RMS axis. In contrast, only 49% ($\pm 3.15\%$) of the neuroblasts moved towards the OB in mutant mice, and many more cells moved toward the SVZ or perpendicular to the RMS ($36\% \pm 2.2\%$ and $15\% \pm 2.15\%$, respectively) during the period of observation (**Fig. 5e**). Cells that were observed to move in different directions also made turns (a turn is defined as a change in direction of $>30^\circ$) during their translocation towards the OB. In contrast to control cells, which made 0.77 ± 0.12 turns per h, ErbB4 mutant cells made 1.8 ± 0.18 turns per h. Taken together, these results suggested that the loss of ErbB4 impaired the orientation and net rate of neuroblast migration in the RMS.

The expression of types I and II and type III NRG1 isoforms in the stream suggested that they could modulate neuroblast migration

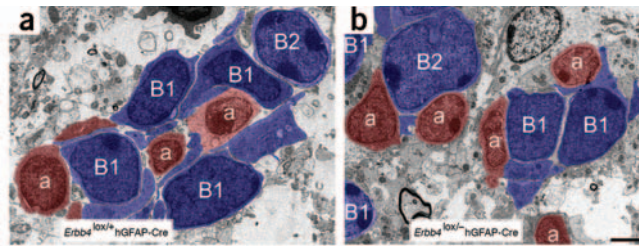


Figure 4 Integrity of glial tubes is disrupted in the RMS after ErbB4 deletion. Electron micrographs of ultrathin coronal sections through the RMS allow for visualization of glial tubes and migrating neuroblasts. (a) In control mice, tightly organized glial tubes, made up of numerous astroglial cell bodies and processes (B1 cells, blue), surround the migrating neuroblasts (A cells, red). (b) In *ErbB4^{lox/+} hGFAP-Cre* mutant mice lacking the ErbB4 receptor, this characteristic organization of glial tubes is disrupted. The number of astroglial processes seems to be less prevalent with fewer direct contacts between B1 type astrocytes. B2 cells are a second type of astrocyte with progenitor-like properties and are distinguishable from B1 cells by their lower cytoplasmic density⁵. Tissue sections were prepared from three adult mice per group. Scale bar, 1.5 μ m.

through ErbB4 by potentially serving as permissive guidance cues, chemotropic agents or motogens. To determine if these isoforms provided a permissive substratum for migration, CMTMR-labeled SVZ explants were placed in between adjacent strips of COS cells expressing NRG1 type I and control (mock-transfected) cells or adjacent strips of COS cells expressing NRG1 type III and control cells. The substrate preference of the neuroblasts migrating out of the SVZ explant was evaluated. SVZ cells had a strong preference for COS cells expressing NRG1 type III, but not for mock-transfected cells or COS cells expressing NRG1 type I (**Fig. 6a–c**). Approximately twice

as many SVZ cells preferred to migrate on cells expressing NRG1 type III than on control substrates (**Fig. 6c**). Similarly, dissociated CMTMR-labeled SVZ cells preferred to adhere to cells expressing NRG1 type III over control cells (**Fig. 6d,e**). ErbB4 mutant SVZ cells did not have a preference for cells expressing NRG1 type III (**Fig. 6b,c**). These results are consistent with the concept that NRG1 type III at the cell surface may provide a permissive, guidance substratum for neuroblast migration towards the OB.

To determine whether secreted NRG1 isoforms had attractive, repulsive or motility-promoting effects during neuroblast migration, we

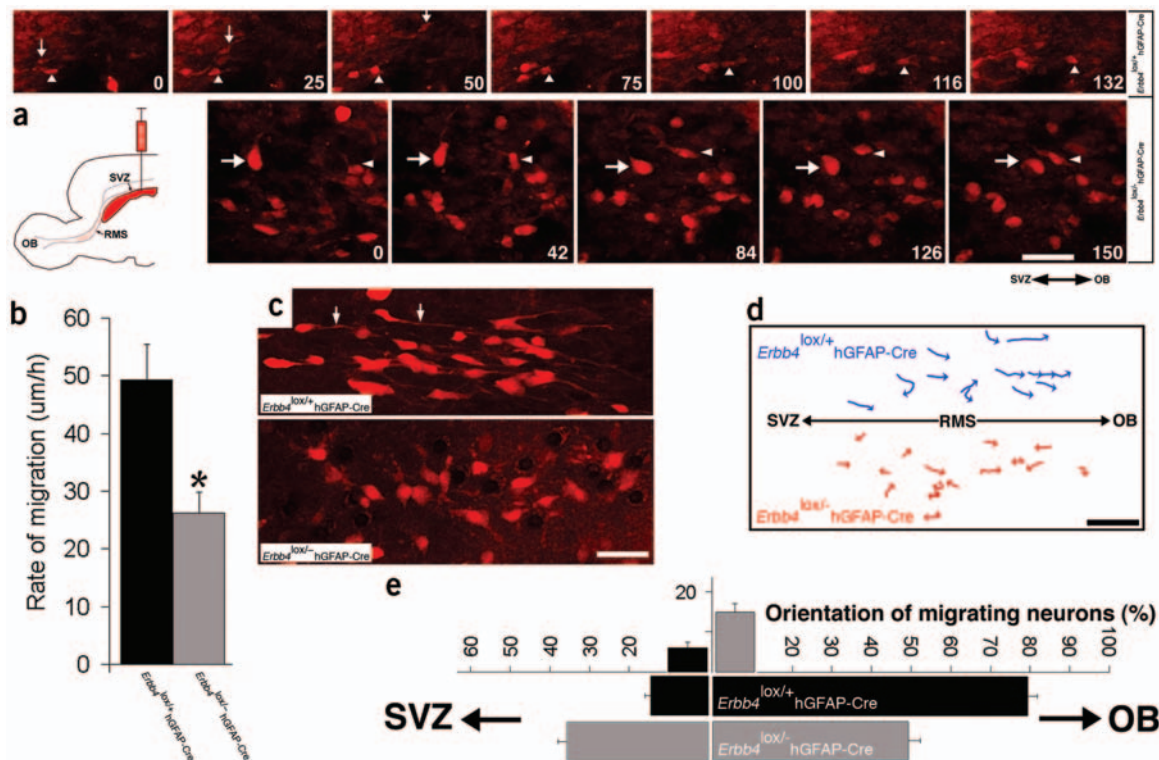


Figure 5 Deficits in the orientation and organization of neuroblast migration in the RMS of ErbB4-deficient mice. (a,b) CMTMR injections into the ventricles were used to label migrating neuroblasts in the RMS. Migration of labeled cells was repeatedly monitored. ErbB4-expressing cells ($n = 244$) migrated robustly at an average rate of $49.29 \pm 6.14 \mu\text{m h}^{-1}$, whereas ErbB4-null cells migrated at a rate of only $26.30 \pm 3.58 \mu\text{m h}^{-1}$ ($n = 210$). Data shown are mean \pm s.e.m.; asterisk, significant compared with controls at $P < 0.01$ (Student's *t*-test). Time elapsed since the beginning of observations is indicated in minutes. See **Supplementary Videos 1 and 2** online. (c,d) Control neuroblasts migrating towards the OB have long leading processes oriented towards the OB (arrows, c). In contrast, ErbB4 mutant cells have processes oriented in multiple different directions (c). (d) Patterns of movement of randomly selected neurons from control and ErbB4-null slices were traced to indicate the general trajectory and orientation of movement during a 1-h period. (e) Quantitative analysis of net orientation of movement of migrating cells indicates that relative to control cells (black bars), mutant cells (gray bars) often migrate in directions away from the OB. (d,e) Arrows in *x* axis identify migration in the direction either towards the SVZ or the OB. Movement in the direction perpendicular to this orientation (either dorsally or ventrally) are charted on the *y* axis and include cells moving towards the surrounding parenchyma. Data shown are mean \pm s.e.m. ($n = 10$); asterisk, significant compared with controls at $P < 0.05$ (Student's *t*-test). Scale bars: a, 45 μ m; c, 30 μ m; d, 100 μ m.

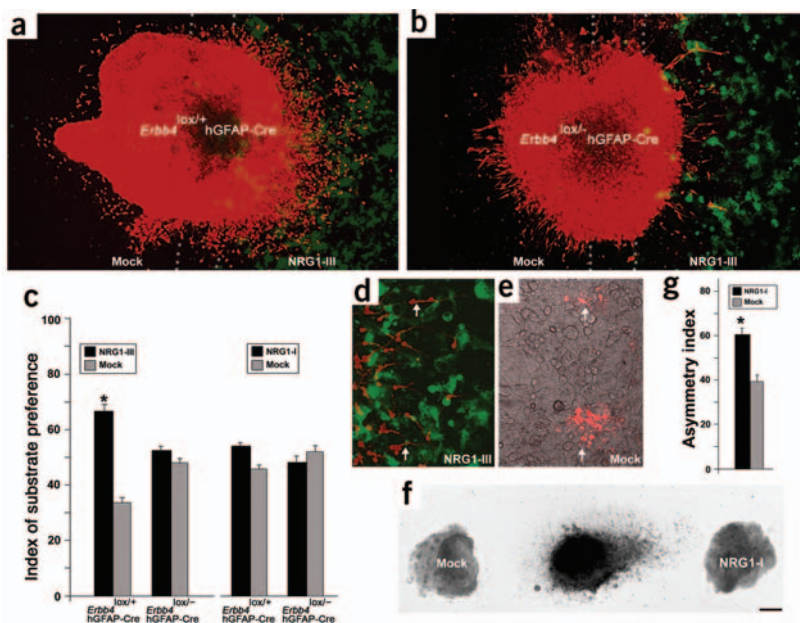


Figure 6 Distinct functions of NRG1 type III and NRG1 type I isoforms *in vitro*. (a–e) SVZ cells prefer substrates expressing NRG1 type III. CMTMR-labeled (red) SVZ explants were placed between strips of COS cells expressing NRG1 type III and mock-transfected cells. Dotted lines indicate the borders of COS cell strips. Cells expressing NRG1 type III were cotransfected with EGFP. Mock-transfected cells are not visible. Control SVZ cells prefer to migrate on the NRG1 type III substrate (a); this preference is abolished in ErbB4 mutant SVZ (*ErbB4*^{lox/-} hGFAP-Cre) cells (b,c). SVZ cells did not show a preference for COS cells expressing NRG1 type I (c). Dissociated, control SVZ cells (arrows in d,e), when seeded onto COS cell strips, adhered preferentially to the NRG1 type III substrate (63% ± 1.2%), rather than to control COS cells (36% ± 2%; d,e). (f,g) NRG1 type I is a chemoattractant for SVZ cells. SVZ explants were placed adjacent to COS cell aggregates expressing NRG1 type I or mock-transfected COS cell aggregates (f). SVZ cells were attracted towards the NRG1 type I source (g). Data shown are mean ± s.e.m. (4 independent experiments); asterisk, significant compared with controls at *P* < 0.01 (Student's *t*-test). Scale bars: a,b, 60 μm; d,e, 90 μm; f, 175 μm.

placed SVZ explants adjacent (~500 μm) to ectopic sources of NRG1 (COS cell aggregates transfected with cDNAs encoding NRG1 type I or type III). The orientation of migration from the SVZ explants relative to NRG1-producing or control COS cell aggregates was evaluated. Most SVZ cells (60.8% ± 2.5%) migrated towards cells expressing NRG1 type I, suggesting that NRG1 type I could function as an attractant or motogen for neuroblast migration *in vivo* (Fig. 6f,g). This potential role as a motogen is consistent with time-lapse observations of chain neuroblast migration from SVZ explants *in vitro*, where the addition of recombinant NRG1β led to a 28% ± 2.3% increase in the rate of migration (E.S.A. & C.L., unpublished observations). Although the ability to serve as a moderate chemoattractant *in vitro* is notable, the *in situ* hybridization profiles of NRG1 types I and II do not identify an obvious source for this factor in the OB.

Defects in OB interneurons in ErbB4-deficient mice

To determine whether the defects observed in the RMS of ErbB4-null mice led to any changes in the generation and placement of interneurons in the OB, we characterized the olfactory interneurons present in the mutant mice, as these cells are believed to arise from SVZ neural stem cells.

Calbindin serves as a marker for interneurons primarily located in the glomerular region³⁰. When compared with controls, *ErbB4*^{lox/-} hGFAP-Cre mice had fewer calbindin-expressing neurons, with 35% fewer positive cells detected in the glomerular layer (Fig. 7a–c). In addition to a change in cell number, the process arborization of the remaining neurons was retarded, suggesting that these cells may differ functionally from their normal counterparts (Fig. 7h–j). ErbB4 mutant cells had fewer branching points per calbindin⁺ neuron (5.4 ± 0.5 versus per 13 ± 1 in controls). The calcium binding protein calretinin, another interneuronal marker, is less restricted in its laminar expression and is normally detected throughout the layers of the bulb. Mutant mice had fewer (15% fewer) calretinin⁺ interneurons in the glomerular layer (Fig. 7d–f). Analysis with the general interneuronal marker GAD65 (glutamic acid decarboxylase-65) showed a 37% decrease in GAD65⁺ interneurons in the glomerular layer (Fig.

7g). Taken together, these findings suggested that the loss of ErbB4 led to a reduction in specific subsets of interneurons.

To further assess the effects of ErbB4 deletion in the migration and final placement of newly born interneurons in the OB, we injected mice with 5-bromodeoxyuridine (BrdU) to label newly generated neuroblasts and collected them one month later for analysis of BrdU⁺ cell position in the OB. Both ErbB4 mutant lines had fewer BrdU⁺ cells in the OB than did controls (Fig. 8a–h and Supplementary Fig. 4 online). The mutants also had altered distribution of these cells, with a significantly reduced percentage located in the glomerular layer and a higher percentage found in the internal granule layer (Fig. 8i). These findings provided support for the idea that ErbB4 is required *in vivo* in the formation and organization of the RMS and olfactory interneurons.

DISCUSSION

In this study, we showed that the receptor protein-tyrosine kinase ErbB4 is expressed by the tangentially migrating neuroblasts in the RMS. We sought to determine whether this expression was indicative of a role for this receptor in regulating the generation, migration and placement of olfactory interneurons. Here we present evidence suggesting that the loss of ErbB4 leads to the formation of an aberrant RMS. ErbB4 mutant neuroblasts in the RMS have a slower rate of migration and deficits in orientation. These defects are correlated with an altered distribution and differentiation of interneurons in the mature OB. These findings imply that ErbB4 has a role in RMS neuroblast migration and olfactory interneuronal placement.

ErbB4 ligands in the RMS

ErbB4 can be activated by at least seven distinct ligands^{14,23}: the neuregulins (NRG1–NRG4), betacellulin, HB-EGF and epiregulin. To identify the possible ErbB4 activators present in the forebrain, we determined the sites of expression of each of these ligands using *in situ* hybridization. This analysis showed that NRG1 was the most readily detected ErbB4 ligand in the SVZ and RMS, with the type III isoform-specific transcripts detected at higher levels than those of the types I and II iso-

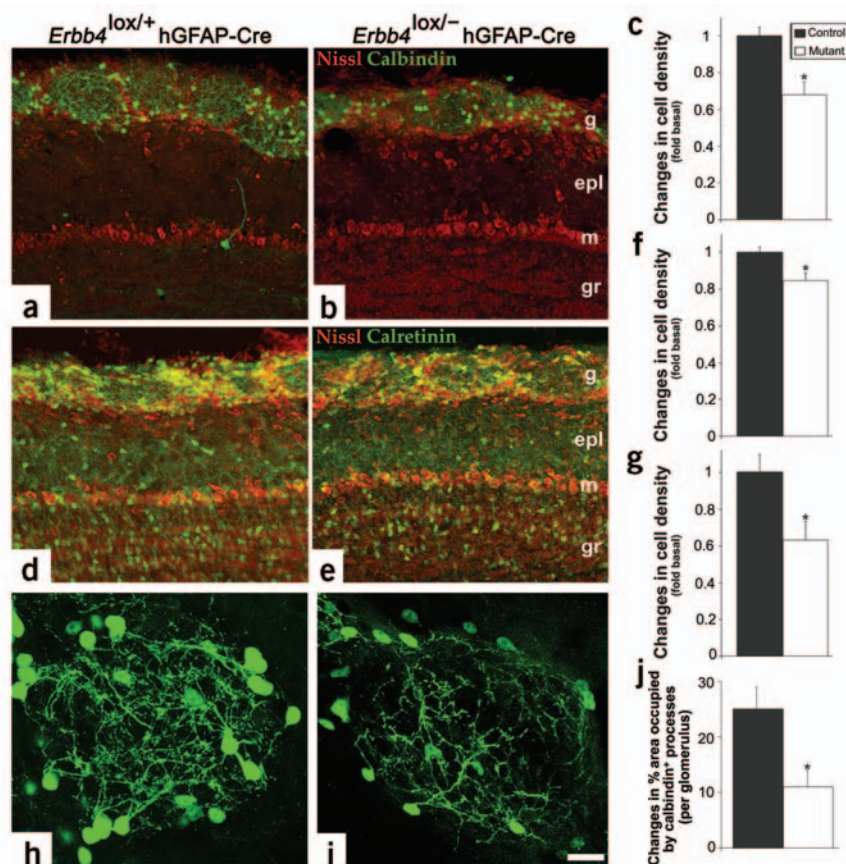


Figure 7 Conditional deletion of ErbB4 reduces the number and alters the differentiation of mature interneurons in the OB. (a) In littermate controls, calbindin is primarily expressed by interneurons in the periglomerular layer, where (d) calretinin is expressed throughout the layers of the OB. (b,c,e–g) Compared with controls, *ErbB4*^{lox/-} hGFAP-Cre mice ($n = 10$) have fewer calbindin⁺ (b,c), calretinin⁺ (e,f) and GAD65⁺ cells (g) in the periglomerular layer. (h–j) Analysis of calbindin⁺ glomeruli showed a substantial reduction in the complexity of the neural process arborization in *ErbB4*^{lox/-} hGFAP-Cre mice ($n = 6$). Data shown are mean \pm s.e.m.; asterisk, significant compared with controls at $P < 0.01$ (Student's t -test). Layers of the OB: G, periglomerular layer; EPL, external plexiform layer; M, mitral cell layer; GR, granule cell layer. Scale bars: a–d, 40 μ m; e,f, 15 μ m.

esis. Other ligands, such as NRG3, which is expressed in regions surrounding the RMS, may serve to restrict or orient migration to this region (Fig. 1i). Oriented neuroblast migration in the adult RMS seems to depend on a combination of repulsive, mitogenic and chemoattractive cues^{31,32}. The combined actions of different NRG isoforms may together provide a permissive substratum and promote the motility of ErbB4-expressing neuroblasts.

The third role for ErbB4 is that it may promote the final placement and influence the differentiation of newly derived interneurons.

The primary finding in support of this concept is that the relative number of GAD65⁺, calbindin⁺ and calretinin⁺ interneurons in the glomerular layer of adult *ErbB4*^{lox/-} hGFAP-Cre mice was reduced. In addition, the dendritic process arborization of calbindin⁺ cells in adult *ErbB4*^{lox/-} hGFAP-Cre mice was severely diminished when compared to controls. How this structural deficit in interneuronal morphology impacts the glomerular synaptic organization and the resultant behavior remains to be elucidated.

It has been previously observed that newly born periglomerular interneurons take ~2–4 weeks to transit from the SVZ to their final destination in the OB³³. Our studies show that one month after BrdU administration to either *ErbB4*^{lox/-} hGFAP-Cre or *ErbB4*^{lox/-} nestin-Cre mice, labeled neurons are more likely to be located in the internal granule layer and less likely to be located in the glomerular layer, compared with littermate controls (Fig. 8). The altered distribution of these newly born cells may reflect a reduced ability of the ErbB4-negative cells to migrate into their appropriate positions in the more superficial layers of the OB. It has been speculated that the tangentially migrating chain neuroblasts in the RMS switch to a radial mode of migration when they reach the OB and start to disperse towards distinct layers. The accumulation of cells at the center of OB, near the region where the RMS ends (Fig. 8g,h), is consistent with the concept that in the absence of ErbB4 signaling, migrating neuroblasts may have additional deficits in transitioning from a tangential to radial mode of migration in the OB. Whether this switch in migratory mode requires radial glial guides is unclear, as the number of radial glia in the adult is very low³⁴. An alternative possibility is that a change in cell fate occurs in migrating ErbB4-negative cells that dictates their final differentiated state and location.

Our studies show that ErbB4 is primarily expressed in PSA-NCAM⁺ neuroblasts but is also detected in a small subset of GFAP⁺ cells, in a

forms. NRG2 was expressed at very low levels in the RMS, and although NRG3 was abundantly expressed in the forebrain, it was not detected in the RMS. These studies showed that there are multiple ligands in the forebrain capable of activating ErbB4 and potentially influencing adult neurogenesis and neuronal chain migration.

Function of ErbB4 in the RMS

Our findings suggest that signaling through ErbB4 has multiple roles. First, ErbB4 is essential for the normal assembly and maintenance of the RMS. Loss of ErbB4 resulted in changes in chain morphology, characterized by the fragmented neuroblast chain organization. In the hGFAP-Cre line, these alterations were associated with a change in the overall gross structure of the stream, which was wider and had a less well-delineated boundary with the surrounding tissue. At the ultrastructural level, the RMS in these mice was readily distinguishable from that in controls, with an apparent loss of cell-cell contact between the migrating A cells, between the A and the B cells, and between the B cells. The loss of ErbB4 also affected neuroblast migration *in vitro*, as SVZ explants prepared from both mutant lines had reduced ability to produce chain-like structures. Together, these observations provide evidence that ErbB4 activity in both nestin⁺ and hGFAP promoter⁺ cells is required for the proper assembly of the RMS.

Second, *in vivo* live imaging of migrating neuroblasts in the RMS indicate that ErbB4 is required for the oriented migration of neuroblasts towards the OB. The disrupted rate and orientation of migration may have resulted from altered neural chain organization. In addition, it could stem from an inability to respond appropriately to environmental cues. The potential mitogenic functions of NRG1 type I and the observed ability of NRG1 type III to act as a preferred migration substrate for normal cells, but not ErbB4 mutant cells, support this hypoth-

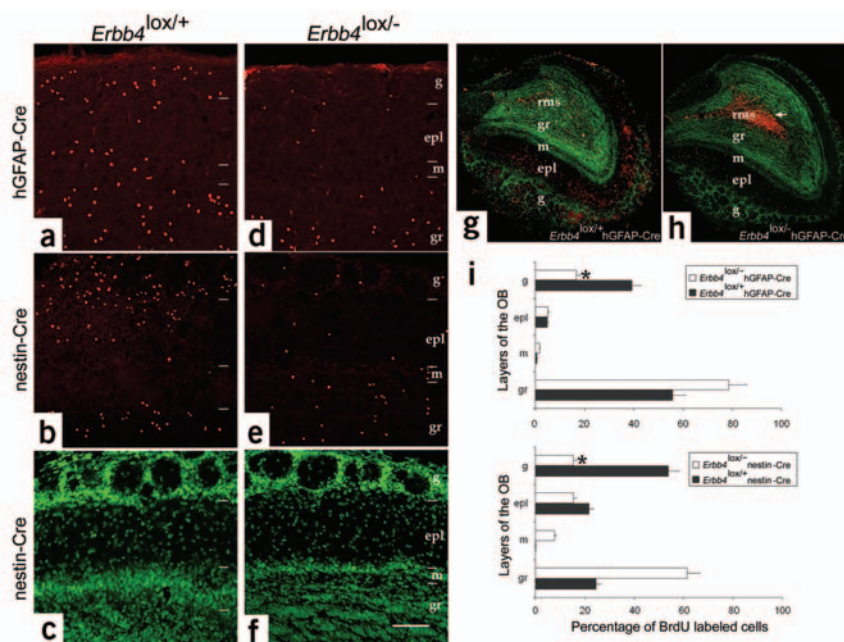


Figure 8 Migration of newly generated cells to the periglomerular layer of the OB is disrupted in ErbB4-deficient mice. Adult *ErbB4*^{lox/-} nestin-Cre and *ErbB4*^{lox/-} hGFAP-Cre mice were given six BrdU injections over a 48-h period and then allowed to survive for 30 d to permit the newly generated neurons to reach their destination in the OB. (a,b) In control mice, BrdU⁺ cells readily migrate and incorporate into the periglomerular layer. (d,e) In mutant mice, BrdU⁺ cells are less prevalent in the target periglomerular layers of the OB and seem to aggregate in the deep granule layer, at the core of the OB (around olfactory ventricular zone). (g,h) In lower-magnification images of the entire cross-section of the OB, accumulation of BrdU⁺ cells (red) in deeper layers, at the center of the mutant OB, is evident (arrow in h). Layers of the OB were delineated using Nissl counterstaining (green in c,f,h). (i) The reduction in the number of BrdU⁺ cells in the periglomerular layer was significant when compared to controls. Data shown are mean \pm s.e.m. ($n = 5$); asterisk, significant compared with controls at $P < 0.01$ (Student's *t*-test). Layers of the OB: G, periglomerular layer; EPL, external plexiform layer; M, mitral cell layer; GR, granule cell layer. Scale bars: a–f, 50 μ m; g,h, 475 μ m.

subset of *dlx-2*⁺ cells and in occasional *LeX*⁺ precursors in the SVZ. Although GFAP has been implicated as a marker of SVZ stem cells, only a tiny fraction of GFAP⁺ cells in this region are believed to serve as stem cells. *dlx-2* seems to mark the rapidly dividing C cells present in the SVZ⁶, which are believed to give rise to the migrating PSA-NCAM⁺ A cells⁵. Thus, although ErbB4 is predominantly expressed in the tangentially migrating cells of the RMS, it is also expressed by other precursor cells in the SVZ.

ErbB4 as a regulator of tangential migration

The expression of ErbB4 in migrating cells has been previously noted in interneuronal precursors that transit from the medial ganglionic eminence to the developing cortex³⁵. ErbB4 has also been detected in migrating neurons that form the basilar pons and inferior olive³⁶. Along with the observations reported here, it seems that ErbB4 is a feature common to tangentially migrating neuroblast populations. Our analyses of ErbB4-deficient mice showed that the loss of this receptor impairs, but does not eliminate, the RMS, implying that this receptor is but one component of the signaling machinery that underlies the migration process. The observed shift from neuroblasts migrating in chains to neuroblasts migrating as individual cells could be the result of changes in the extracellular matrix or in the adhesive properties of migrating cells³². The loss of ErbB4 may alter signaling through other receptor systems, such as the integrins, which have been previously shown to regulate the differentiation and migration of RMS neuroblasts^{37–39}. There is evidence for crosstalk between ErbB and integrin signaling pathways, as the integrins can switch NRG responsiveness in glioblasts from proliferation to differentiation⁴⁰.

In addition to integrins³⁹, changes in the structure of the RMS have been shown in response to the loss of polysialic acid residues from PSA-NCAM, which results in the dispersion of migrating neuroblasts both *in vivo* and *in vitro*^{32,41}. Another molecule influencing RMS function is Reelin, which has a role in the dispersal of neuroblasts in the OB *in vivo* and can disrupt the chain-like migration of SVZ cells *in vitro*⁴² in a manner similar to that seen in explants from the ErbB4 mutant mice. Although the extracellular matrix molecule tenascin-R does

not influence RMS migration, it facilitates the transition from tangential to radial migration as cells leave the RMS and enter the OB⁴³. Furthermore, Eph-ephrin signaling and other extracellular activities have been implicated as modifiers of tangential migration in the RMS^{31,32}. Finally, ErbB4 has been recognized as the first receptor tyrosine kinase whose C-terminal region is released by intramembrane proteolysis⁴⁴. The ErbB4 cytoplasmic tail, including the catalytic domain, has been shown to enter the nucleus, where it may influence transcription⁴⁴. Thus, it is conceivable that ErbB4 might help to regulate migration and differentiation by directly mediating changes in gene expression.

Overall, our findings suggest that ErbB4 activation may help to regulate the migration of precursors in the RMS and may influence their placement and differentiation into distinct interneuronal subsets. The regulation of both differentiation and migration by the same receptor may permit the targeted placement of specific neuronal types in the mature brain. The identification of the physiologically relevant endogenous ErbB4 ligands will be essential to evaluate further the comparative importance of ErbB4 signaling in adult forebrain neurogenesis. Notably, mice heterozygous with respect to either *Nrg1* or *ErbB4* have behavioral phenotypes that model those associated with schizophrenia⁴⁵. Recent studies identifying *NRG1* as a gene associated with susceptibility to schizophrenia⁴⁵ raise the possibility that impaired NRG-ErbB4-mediated neuronal precursor differentiation and migration, and the resultant changes in neural circuitry in the forebrain, may enhance sensitivity to neurodevelopmental disorders such as schizophrenia.

METHODS

In situ hybridization; antibodies and histology; NRG1 cDNA clones. *In situ* hybridization was carried out as previously described⁴⁶, with minor modifications. Details concerning the antibodies, *in situ* hybridization probes, immunohistological methods and full-length *NRG1* cDNA clones that we used are provided in **Supplementary Methods** online.

Mice. Mice were cared for according to animal protocols approved by The Scripps Research Institute and the University of North Carolina. Nervous sys-

tem-specific conditional knockout *ErbB4* mice were generated by mating mice carrying an *ErbB4* allele flanked by *loxP* sites²⁴ with either nestin-Cre mice²⁶ or hGFAP-Cre mice²⁸. Additional details are available in **Supplementary Methods** online.

SVZ explant migration assays. This assay was based on described methods²⁹. See **Supplementary Methods** online for details.

Analysis of BrdU⁺ cell distribution in the OB. To study the effects of *ErbB4* deletion on the final positioning of newly generated cells into the OB, we injected adult mice with BrdU (100 mg per kg body weight, three times per day) over a period of 48 h and collected them 30 d after the final injection. See **Supplementary Methods** online for details of analysis of BrdU⁺ cell distribution in the OB.

Analysis of neuroblast migration and orientation in the RMS. We injected 1 µl of 40 µM CMTMR ((5-(and-6)-((4-chloromethyl)benzoyl) amino) tetramethyl rhodamine); Molecular Probes) into the anterior ventricles of 3-week-old control (*n* = 10) and *ErbB4*-deficient (*n* = 10) mice. After 4–6 h, the brains were removed, sectioned in the sagittal plane (100 µm) using a vibratome (Leica), mounted on nucleopore membrane filters and maintained in minimal essential medium with 10% fetal bovine serum at 37 °C and 5% CO₂. The CMTMR-labeled cells migrating from the SVZ into the RMS were repeatedly imaged at intervals of 5–10 min for 2–3 h using a Zeiss Pascal laser scanning confocal microscope equipped with a live-cell incubation chamber. The rate and orientation of migration (towards the OB, the surrounding parenchyma or the SVZ) were quantified as previously described⁴⁷.

Analysis of chemotropic or guidance role of NRG1. To determine whether NRG1 type I or type III isoforms provided a permissive substratum for migration, we gave neuroblasts emigrating from SVZ explants a choice between normal or NRG1-expressing COS cell substrates and quantified the substrate preference of migrating SVZ cells. See **Supplementary Methods** online for details. In some experiments, dissociated CMTMR-labeled SVZ cells were seeded onto COS cell substrates at a density of 50,000 cells ml⁻¹. After 24 h, the percentage of CMTMR-labeled SVZ cells on each substrate was quantified.

To determine possible chemoattractive or repulsive effects of the NRG1 isoforms, explants were placed adjacent (500 µm) to ectopic sources of NRG1 (COS cell aggregates transfected with NRG1 isoforms) or untransfected COS cell aggregates, and the orientation of migration from the explants towards or away from these sources was evaluated to determine their attractive or repulsive effects. The asymmetry index is defined as the percentage of outgrowth towards each of the two COS cell aggregates, which were made as previously described⁴⁸.

Analysis of olfactory periglomerular layer interneurons. The numbers of calbindin⁺, calretinin⁺ and GAD65⁺ cells in the periglomerular layer of the OB were estimated using the optical fractionator method⁴⁹. Total numbers of calbindin⁺ or calretinin⁺ cells per unit volume (mm³) in the periglomerular layer of *ErbB4* mutant mice (*n* = 10) were normalized to the values from controls (*n* = 10). The analysis of olfactory glomerular processes is provided in **Supplementary Methods** online.

Analysis of process arborization in olfactory glomeruli. See **Supplementary Methods** online for details.

Note: Supplementary information is available on the Nature Neuroscience website.

ACKNOWLEDGMENTS

We thank H.G. Kuhn for his insight and encouragement, A.-S. Lamantia, L. Pevny, F. Polleux, G. Haskell, N. Sestan and R. Schmid for comments and O. Marin for communicating his unpublished observations prior to publication. This work was supported by grants from the US National Institutes of Health to C.L. and E.A. (NS39411) and by the March of Dimes foundation to E.A. Core 5 of an NINDS-funded Center grant (P30NS045892) was used to generate some of the images.

COMPETING INTERESTS STATEMENT

The authors declare that they have no competing financial interests.

Received 11 June; accepted 30 August 2004

Published online at <http://www.nature.com/natureneuroscience/>

- Alvarez-Buylla, A., Seri, B. & Doetsch, F. Identification of neural stem cells in the adult vertebrate brain. *Brain Res. Bull.* **6**, 751–758 (2002).
- Gage, F.H. Neurogenesis in the adult brain. *J. Neurosci.* **22**, 612–613 (2002).
- Kornack, D.R. & Rakic, P. The generation, migration, and differentiation of olfactory neurons in the adult primate brain. *Proc. Natl. Acad. Sci. USA* **98**, 4752–4757 (2001).
- Luskin, M.B. Restricted proliferation and migration of postnatally generated neurons derived from the forebrain subventricular zone. *Neuron* **11**, 173–189 (1993).
- Doetsch, F., Garcia-Verdugo, J.M. & Alvarez-Buylla, A. Cellular composition and three-dimensional organization of the subventricular germinal zone in the adult mammalian brain. *J. Neurosci.* **17**, 5046–5061 (1997).
- Doetsch, F., Petranu, L., Caille, I., Garcia-Verdugo, J.M. & Alvarez-Buylla, A. EGF converts transit-amplifying neurogenic precursors in the adult brain into multipotent stem cells. *Neuron* **36**, 1021–1034 (2002).
- Capela, A. & Temple, S. LeX/SSEA-1 is expressed by adult mouse CNS stem cells, identifying them as non-ependymal. *Neuron* **35**, 865–875 (2002).
- Morshead, C.M. *et al.* Neural stem cells in the adult mammalian forebrain: a relatively quiescent subpopulation of subependymal cells. *Neuron* **13**, 1071–1082 (1994).
- Gregg, C.T., Shingo, T. & Weiss, S. Neural stem cells of the mammalian forebrain. *Symp. Soc. Exp. Biol.* **53**, 1–19 (2001).
- Anderson, M.F., Aberg, M.A., Nilsson, M. & Eriksson, P.S. Insulin-like growth factor-I and neurogenesis in the adult mammalian brain. *Brain Res. Dev. Brain Res.* **134**, 115–122 (2002).
- Shingo, T., Sorokan, S.T., Shimazaki, T. & Weiss, S. Erythropoietin regulates the *in vitro* and *in vivo* production of neuronal progenitors by mammalian forebrain neural stem cells. *J. Neurosci.* **15**, 9733–9743 (2001).
- Tropepe, V., Craig, C.G., Morshead, C.M. & van der Kooy, D. Transforming growth factor- α null and senescent mice show decreased neural progenitor cell proliferation in the forebrain subependyma. *J. Neurosci.* **17**, 7850–7859 (1997).
- Sibilia, M., Steinbach, J.P., Stingl, L., Aguzzi, A. & Wagner, E.F. A strain-independent postnatal neurodegeneration in mice lacking the EGF receptor. *EMBO J.* **17**, 719–731 (1998).
- Yarden, Y. & Sliwkowski, M.X. Untangling the ErbB signalling network. *Nat. Rev. Mol. Cell Biol.* **2**, 127–137 (2001).
- Buonanno, A. & Fischbach, G.D. Neuregulin and ErbB receptor signaling pathways in the nervous system. *Curr. Opin. Neurobiol.* **11**, 287–296 (2001).
- Hippenmeyer, S. *et al.* A role for neuregulin1 signaling in muscle spindle differentiation. *Neuron* **36**, 1035–1049 (2002).
- Garratt, A.N., Britsch, S. & Birchmeier, C. Neuregulin, a factor with many functions in the life of a Schwann cell. *Bioessays* **22**, 987–996 (2000).
- Michailov, G.V. *et al.* Axonal neuregulin-1 regulates myelin sheath thickness. *Science* **304**, 700–703 (2004).
- Corfas, G., Rosen, K.M., Aratake, H., Krauss, R. & Fischbach, G.D. Differential expression of ARIA isoforms in the rat brain. *Neuron* **14**, 103–115 (1995).
- Anton, E.S., Marchionni, M.A., Lee, K.-F. & Rakic, P. Role of GGF/neuregulin signaling in interactions between migrating neurons and radial glia in the developing cerebral cortex. *Development* **124**, 3501–3510 (1997).
- Rio, C., Rieff, H.I., Qi, P., Khurana, T.S. & Corfas, G. Neuregulin and erbB receptors play a critical role in neuronal migration. *Neuron* **19**, 39–50 (1997).
- Schmid, R.S. *et al.* Neuregulin 1-erbB2 signaling is required for the establishment of radial glia and their transformation into astrocytes in cerebral cortex. *Proc. Natl. Acad. Sci. USA* **100**, 4251–4256 (2003).
- Riese, D.J. 2nd & Stern, D.F. Specificity within the EGF family/ErbB receptor family signaling network. *Bioessays* **20**, 41–48 (1998).
- Golub, M.S., Germann, S.L. & Lloyd, K.C.K. Behavioral characteristics of a nervous system-specific erbB4 knock-out mouse. *Behav. Brain Res.* **153**, 159–170 (2004).
- Gassmann, M. *et al.* Aberrant neural and cardiac development in mice lacking the ErbB4 neuregulin receptor. *Nature* **378**, 390–394 (1995).
- Tronche, F. *et al.* Disruption of the glucocorticoid receptor gene in the nervous system results in reduced anxiety. *Nat. Genet.* **23**, 99–103 (1999).
- Graus-Porta, D. *et al.* Beta1-class integrins regulate the development of laminae and folia in the cerebral and cerebellar cortex. *Neuron* **31**, 367–379 (2001).
- Zhuo, L. *et al.* hGFAP-cre transgenic mice for manipulation of glial and neuronal function *in vivo*. *Genesis* **31**, 85–94 (2001).
- Wichterle, H., Garcia-Verdugo, J.M. & Alvarez-Buylla, A. Direct evidence for homotypic, glia-independent neuronal migration. *Neuron* **18**, 779–791 (1997).
- Kawaguchi, Y. & Kubota, Y. GABAergic cell subtypes and their synaptic connections in rat frontal cortex. *Cereb. Cortex* **7**, 476–486 (1997).
- Mason, H.A., Ito, S. & Corfas, G. Extracellular signals that regulate the tangential migration of olfactory bulb neuronal precursors: inducers, inhibitors, and repellants. *J. Neurosci.* **21**, 7654–7663 (2001).
- Marin, O. & Rubenstein, J.L.R. Cell migration in the forebrain. *Ann. Rev. Neurosci.* **26**, 441–483 (2003).
- Lois, C. & Alvarez-Buylla, A. Long-distance neuronal migration in the adult mammalian brain. *Science* **264**, 1145–1148 (1994).
- Chiu, K. & Greer, C.A. Immunocytochemical analyses of astrocyte development in the olfactory bulb. *Dev. Brain Res.* **95**, 28–37 (1996).
- Yau, H.J., Wang, H.F., Lai, C. & Liu, F.-C. Neural development of the neuregulin receptor ErbB4 in the cerebral cortex and the hippocampus: preferential expression by interneurons tangentially migrating from the ganglionic eminences. *Cereb. Cortex* **13**, 252–264 (2003).



36. Yee, K.T. & O'Leary, D.D.M. Migrating basilar pontine and inferior olive neurons express erbB4. *Abstr. Soc. Neurosci.* **692.7** (2001).
37. Jacques, T.S. *et al.* Neural precursor cell chain migration and division are regulated through different beta1 integrins. *Development* **125**, 3167–3177 (1998).
38. Murase, S. & Horwitz, A.F. Deleted in colorectal carcinoma and differentially expressed integrins mediate the directional migration of neural precursors in the rostral migratory stream. *J. Neurosci.* **22**, 3568–3579 (2002).
39. Emsley, J.G. & Hagg, T. Alpha6beta1 integrin directs migration of neuronal precursors in the adult mouse forebrain. *Exp. Neurol.* **183**, 273–285 (2003).
40. Cognato, H. *et al.* CNS integrins switch growth factor signalling to promote target-dependent survival. *Nat. Cell Biol.* **4**, 833–841 (2002).
41. Chazal, G., Durbec, P., Jankovski, A., Rougon, G. & Cremer, H. Consequences of neural cell adhesion molecule deficiency on cell migration in the rostral migratory stream of the mouse. *J. Neurosci.* **20**, 1446–1457 (2000).
42. Hack, I., Bancila, M., Loulier, K., Carroll, P. & Cremer, H. Reelin is a detachment signal in tangential chain-migration during postnatal neurogenesis. *Nat. Neurosci.* **5**, 939–945 (2002).
43. Saghatelian, A., de Chevigny, A., Schachner, M. & Lledo, P.M. Tenascin-R mediates activity-dependent recruitment of neuroblasts in the adult mouse forebrain. *Nat. Neurosci.* **4**, 347–356 (2004).
44. Carpenter, G. ErbB-4: mechanism of action and biology. *Exp. Cell Res.* **284**, 66–77 (2003).
45. Stefansson, H. *et al.* Neuregulin 1 and susceptibility to schizophrenia. *Am. J. Hum. Genet.* **71**, 877–892 (2002).
46. Simmons, D.M., Arriza, J.L. & Swanson, L.W. A complete protocol for *in situ* hybridization of messenger RNAs in brain and other tissues with radiolabeled single-stranded RNA probes. *J. Histochem. J.* **12**, 169–181 (1989).
47. Gongidi, V., Ring, C., Rakic, P. & Anton, E.S. Sparc-like 1 is a radial glia-associated terminator of neuronal migration in cerebral cortex. *Neuron* **41**, 57–69 (2004).
48. Zhu, Y., Li, H., Zhou, L., Wu, J.Y. & Rao, Y. Cellular and molecular guidance of GABAergic neuronal migration from an extracortical origin to the neocortex. *Neuron* **23**, 473–485 (1999).
49. West, M. J. & Gundersen, H.J. Unbiased stereological estimation of the number of neurons in the human hippocampus. *J. Comp. Neurol.* **296**, 1–22 (1990).